Songklanakarin J. Sci. Technol.
44 (2), 517-523, Mar. - Apr. 2022

http://www.sjst.psu.ac.th

Original Article

Using design of experiments to fabricate nanostructured lipid carrier of egg white hydrolysates

Nisachon Jangpromma[1], Supisara Jearranaiprepame[2], Boonpob Nowichai[1], Sirinthip Sosiangdi[1], and Watcharee Khunkitti[2*]

[1] *Protein and Proteomics Research Center for Commercial and Industrial Purposes, Khon Kaen University, Mueang, Khon Kaen, 40002 Thailand*

[2] *Department of Pharmaceutical Technology, Faculty of Pharmaceutical Science, Khon Kaen University, Mueang, Khon Kaen, 40002 Thailand*

Received: 21 August 2021; Revised: 23 September 2021; Accepted: 19 October 2021

Abstract

The aims of this study were to develop a nanostructured lipid carrier (NLC) system and optimize an appropriate NLC formulation using design of experiments (DOE). The results showed that the formulation containing glycerol monostearate (GMS) 0.35 g, stearic acid (SA) 0.50 g and isopropyl myristate (IPM) 0.65 g was optimal with entrapment efficiency (%EE) (59.21%), particle size (233.7nm) and zeta potential (-41.26 mV). Moreover, solid lipid (GMS, SA) and liquid lipid (IPM) had significant impact on NLC characteristics. The positive effect on the %EE was due to the interaction between GMS and IPM, and SA and IPM. The optimal formulation EWH-NLC at concentration 125 µg/ml expressed the highest inhibitory activity against NO production in RAW 264.7 macrophages with no cytotoxicity. The release profile of EWH-NLC in the cream base exhibited sustained release behavior that best fitted with Higuchi model. These results suggest that the NLC is a suitable carrier for EWH in topical application with a sustained-release profile.

Keywords: nanostructured lipid carriers, design of experiment, egg white hydrolysates, delivery, skin barrier

1. Introduction

Hen egg white is also known as an excellent source of high-quality proteins and bioactive peptides. In our previous study, protein hydrolysates from egg white aided the wound healing process via anti-inflammatory mechanism, cell proliferation and migration, and collagen synthesis (Jearranaiprepame, Jangpromma, & Khunkitti, 2019). However, these peptides represent hydrophilic and high molecular weights substances (around 3.5 kDa) that cannot be transported across the cutaneous barrier of the skin. To enhance penetration of the substance through the skin, nanocarriers can be used as an effective delivery system (Shah, Desai, Channer, & Singh, 2012).

*Corresponding author
Email address: watkhu@kku.ac.th; watkhu@yahoo.com

Nanostructured lipid carriers (NLCs) are the lipid nanoparticles containing solid and liquid lipids that create a partially crystalized lipid matrix with improved drug loading capacity (Jia et al., 2010). NLCs with a particle size being in the range 10-1000 nm have emerged as one of the promising drug delivery systems of pharmaceuticals particularly for transdermal route. The smaller size NLCs increase a surface contact with the stratum corneum and increase the amount of the active compound delivery through the skin (Li & Ge, 2012). Moreover, NLCs improve skin hydration and exhibit occlusive properties due to reduction in the trans-epidermal water loss (Loo et al., 2013). In addition, it has ability to protect substances from degradation, increase drug loading capacity in the particles, prevent drug expulsion during storage, good biocompatibility, low cytotoxicity, as well as reduce skin irritation. (Czajkowska-Kośnik, Szekalska, & Winnicka, 2019).

Design of experiment (DOE) is an efficient procedure used in formulation development by employing a statistics based modeling that requires fewer formulations than trial and error method, saving the time and cost. In this study, Plackett-Burman design was used in the early stages of experiments to screen and narrow down the potential important factors that influenced characteristics of NLCs. When important factors were identified, mixture design was used to optimize the relative proportions of factors contributing to the properties of NLCs. Therefore, the aims of this study were to develop a nanostructured lipid carrier system and optimize an appropriate NLC formulation using experimental design.

2. Materials and Methods

Hen eggs were obtained from Polwittaya Farm (Khon Kaen, Thailand). All analytical chemicals were purchased from Sigma-Aldrich (MO, USA). All other ingredients e.g. glyceryl monosterate (GMS), stearic acid (SA), cetyl alcohol (CA), isopropyl myristate (IPM) were obtained from S. Tong Chemicals Co., Ltd. (Nonthaburi, Thailand).

2.1 Preparation of egg white hydrolysates

Crude egg white was mixed with 0.4 M KOH at a ratio of 1:3. The mixture was hydrolyzed in water bath at 55 °C for 2 hrs and then autoclaved at 121 °C 15 psi for 2 hrs. The hydrolysates were filtered twice through five layers of gauze. The filtrate was then collected and adjusted to pH 7.0 using hydrochloric acid. Finally, egg white hydrolysates (EWH) were dried by lyophilization and stored in freezer at -40 °C.

2.2 Design of experiment

2.2.1 Screening of factors affecting EWH nanostructured lipid carrier (EWH-NLC) characteristics using Plackett-Burman design

Six independent factors at low and high levels were investigated. The response variables were Y_1 (%entrapment efficiency), Y_2 (particle size) and Y_3 (zeta potential) (Table 1). Design layout of NLCs formulations and responses using Plackett-Burman design are shown in Table 2.

2.2.2 Preparation of EWH-NLC

EWH-NLC was prepared using multiple emulsion method. All compositions are shown in Table 1. In brief, the solid lipids (GMS, SA, CA) and the liquid lipid (IPM) were melted together in a 250-ml beaker at 70 °C in the water bath. Span 80 and EWH (0.1 g) were added in the mixture and stirred at 750 rpm for 1 min using a mixer (C-MAG HS7-IKA, IKA® Works (Thailand) Co. Ltd) until the primary emulsion was formed. Primary emulsion was sonicated in 45 °C at 59 kHz for 20 sec. Tween 80 and 200 µl of water was then added and stirred at 750 rpm for 3 min until the secondary emulsion was formed. Secondary emulsion was sonicated for 1 min and transferred into cold water (5-8 °C) with continuous stirring at 750 rpm for 5 min.

Table 1. Screening of factors affecting the nanostructured lipid carrier formulations using Plackett-Burman design

Independent variable	Level used (coded)	
	Low (-1)	High (1)
A = Glyceryl monostearate (GMS)	0	0.3
B = Stearic acid (SA)	0	0.3
C = Cetyl alcohol (CA)	0	0.3
D = Isopropyl myristate (IPM)	0.3	0.6
E = Polysorbate 80 (Tween 80)	0	6
F = Sorbitan monooleate (Span 80)	0	0.6

Table 2. Composition of EWH-NLC and cream base

Ingredients	Amount (g)
EWH-NLC	
EWH	0.1
Glyceryl monostearate (GMS)	A
Stearic acid (SA)	B
Cetyl alcohol (CA)	C
Isopropyl Myristate (IPM)	D
Sorbitan oleate (Span80)	E
Polysorbate 80 (Tween80)	F
DI water part I	0.2 (200µl)
DI water for solidification (cold water)	100-(X+0.2+0.1)
Total	100
Cream base	
Mineral oil (g)	30
Ceteareth-20 (Cetomacrogol 1000) (g)	10
Triethanolamine (TEA) (g)	0.4
Carbomer 940 (Carbopol 940) (g)	0.5
Glycerin (g)	5
Propylene Glycol and Diazolidinyl Urea and Methylparaben and Propylparaben (Unigerm G-2) (g)	1
Deionized water qs. to	100

A-F: Variable factors; X was total amount of A-F.

2.2.3 Entrapment efficiency

EWH-NLC (1 mL) was centrifuged at 13420 xg for 4 hrs at 4 °C (Kubota 6200, Japan). The precipitate was collected and washed with DI water. 500 µL acetone was added to dissolve the shell of NLC and centrifuged at 13420 xg for 15 min at 4 °C. The supernatant was mixed with 500 µL of DI water. The total protein of sample was determined using Bradford protein assay and %EE was calculated by the equation (1):

$$\% \text{ Entrapment effiency} = \frac{\text{Amount of entrapped EWH}}{\text{Amount of total EWH}} \times 100 \quad (1)$$

where the amount of entrapped EWH is the total protein of EWH entrapped in NLC, and the amount of total EWH is the total protein of EWH added in the system.

2.2.4 Particle size

EWH-NLC samples were diluted with ultrapure water at a ratio of 1:25 (NLC:water). Then 1,000 µL aliquot of sample was pipetted to polystyrene cell (Brand, Germany).

Particle sizes were reported as Z-average. The mean particle size of EWH-NLC was measured using Nano S90 Zetasizer (Malvern instruments Ltd., UK).

2.2.5 Zeta potential

The samples were diluted with ultrapure water at a ratio of 1:25 (NLC: water). Then 1,000 µL aliquots of samples were pipetted to disposable folded capillary cells (Malvern instruments Ltd., UK). Each sample was measured in triplicate at 25 °C.

2.2.6 Optimization of data and model validation

Based on preliminary experiments, the significant independent variables affecting the formulation of EWH-NLC were selected and optimized to obtain maximum %EE, minimum particle size and high different value of zeta potential. The response variables in optimization were Y_1 (%entrapment efficiency), Y_2 (particle size) and Y_3 (zeta potential). Selected parameters were evaluated using simplex-centroid mixture design.

Validation process was performed to assess reliability of model for optimization process. Based on the results and overlay plot from the optimization process, formulations represented by four points in optimized area were selected and prepared and evaluated for %EE, particle size and zeta potential values that were further compared with the prediction values by Design-Expert® 7.1 software (Stat-Ease Inc., Minneapolis, USA). The % prediction error was calculated by equation (2):

$$\% \text{ Prediction error} = \frac{\text{Measurement value} - \text{predicted value}}{\text{Predicted value}} \times 100 \quad (2)$$

If % prediction error was ≤10%, it confirmed that this model was reliable for the optimization process.

2.2.7 Anti-inflammation activity using nitric oxide inhibition assay

The nitric oxide inhibition assay was determined in murine macrophage cell line RAW 264.7. The cells were seeded into a sterile 96 well-plate at 5 x 10^4 cells/well and cultured at 37 °C with 5% CO_2/95% relative humidity. Cells used in this experiment were divided into three groups: untreated cells replaced with medium contained only 1% (v/v) antibiotic-antimycotic solution; cells treated with RPMI 1640 medium containing 100 ng/ml of lipopolysaccharides (LPS) and cells treated with medium contained LPS (100 ng mL^{-1}) together with the test samples (EWH-NLC and empty NLC) at various concentrations. Cells were incubated at 37 °C with 5% CO_2/95% RH for 24 hrs. The nitric oxide inhibition assay was evaluated by measuring nitrite in the supernatants of RAW 264.7 cell culture. NO reduction was determined by mixing 100 µl of the sample with 100 µl of Griess reagent containing 2% (w/w) sulfanilamide and 2% (w/w) N-1-**[**naphthyl**]** ethylenediamine dihydrochloride in 4% (w/w) H_3PO_4. The absorbance of the solution was evaluated after 10 min by Varioskan flash microplate reader (Thermo Fisher, Finland) at 540 nm. The % nitric oxide production was calculated using equation (3):

$$\% \text{ Nitric oxide production} = \frac{(Abs_{sample})}{(Abs_{control})} \times 100 \quad (3)$$

where $Abs_{control}$ is the absorbance of cells treated with medium contained LPS, and Abs_{sample} is the absorbance of cells treated with sample and medium contained LPS.

The cell viability was measured using Prestoblue® mixture (50 µl) (Sigma-Aldrich, USA) prepared as 1:9 parts of Prestoblue®:cell medium. The plate was incubated at 37 °C with 5% CO_2/95% RH for 90 min. The mixture was then determined by Verioskan flash microplate reader (Thermo Fisher, Finland) at wavelengths 560 nm/590 nm. The results were reported as %cell viability calculated using equation (4) (Fischer, Li, Ahlemeyer, Krieglstein, & Kissel, 2003:

$$\% \text{ Cell viability} = \frac{Abs_{sample}}{Abs_{control}} \times 100 \quad (4)$$

where $Abs_{control}$ is the absorbance of cells treated with medium at 0 h; Abs_{sample} is the absorbance of cells treated with EWH at the time intervals.

2.2.8 *In vitro* drug release studies

In vitro release studies were determined using Franz diffusion cell. The EWH-NLC contained 10 mg/mL of total protein or EWH were incorporated in cream base showed in Table 2. Cream base (1 g) was applied on 0.2 µm cellulose acetate membrane filter. The receptor compartments were filled with phosphate buffer (pH 7.4). The temperature of the cell was maintained at 37 °C by circulating water bath. Aliquots of samples (300 µl) in the receptor compartments were collected at predetermined time for 720 min. Once the samples were collected, the equal volume of freshly prepared PBS buffer was immediately added to the receptor phase. Total protein release in the aliquots of samples was determined. The cumulative protein release profiles were generated and fitted to different release kinetics models.

2.2.9 Bradford protein assay

The total protein of EWH was evaluated using Bradford protein assay (Bradford, 1976). A solution of ovalbumin (OVA) in different concentrations was used to prepare a standard curve. Twenty microliters of samples were pipetted into 96-well plate and 180 µL of Bradford dry reagent was added and kept at 25 °C for 5 min. The absorbance of the mixture was measured at 595 nm by UV-Visible spectrophotometer and the total protein of EWH was calculated.

2.2.10 Statistical analysis

All experiments were performed in triplicates. The results were expressed as the mean ± SD. Statistical analysis was performed by Design-Expert® 7.1 software (Stat-Ease Inc., Minneapolis, USA), and analysis of variance (ANOVA) was conducted to determine the significance of the studied parameters. A p-value of <0.05 was considered statistically significant.

3. Results

3.1 Screening parameters using Plackett-Burman design

Plackett-Burmann design was used to screen formulation factors by applying statistical methods and evaluate effects influencing entrapment efficiency (%EE), particle size and zeta potential. The R^2 values were 0.7868, 0.9969 and 0.9602 for Y_1 (%EE), Y_2 (particle size) and Y_3 (zeta potential), respectively. All response models were statistically significant ($p<0.05$), indicating that the relationship between the variables and responses was well described by this model. The linear model equations in term of coded levels for three responses are as follows:

$$Y1 = +27.47 + 95.49A^* + 39.31F \quad (5)$$

$$Y2 = +451.28 - 252.29A^* + 242.29D^* - 255.21F^* \quad (6)$$

$$Y3 = -10.82 + 1.01E^* - 15.13F^* \quad (7)$$

Results indicated that GMS (A) had a significant positive influence on %EE suggesting that %EE escalated with the increase of the GMS amount in formulation. GMS and Span 80 showed a significant negative effect on the particle size meaning that with the increase of GMS and Span 80, the particle size decreased. An increase of IPM, in the opposite way, caused significantly increased particle size. Both surfactants, including Tween 80 and Span 80 had significantly negative effect on zeta potential. As the concentrations of surfactants increased, zeta potential changed to more negative value resulting in zeta potential lower than -30 mV. As a result, the EWH-NLC increased % EE, reduced particle size (100-500 nm) and caused high zeta potential (more negative than -30 mV) with the increase of concentration of GMS, Tween 80, Span 80 and decrease of concentration of IPM. Accordingly, these four parameters were selected for the optimization study to develop appropriate EWH-NLC formulations.

3.2 Optimization of EWH-NLC formulation

The formulation optimization using simplex-centroid mixture design found that Tween 80 and Span 80 could not be used for prediction by this model since the values of both parameters were out of range for GMS and IPM. Thus, SA was selected for optimization instead. Other compositions in formulation optimization were prepared by using the same amount as formulation 1 from Plackett-Burman design (Table 3). Quadratic models were selected for analysis of %EE and particle size, while zeta potential was analyzed by linear models. The model predicted for %EE showed statistical significance. The lack of fit was not significant. The R^2 value was 0.8766. Therefore, this model can be used to navigate the design space, whereas the models for particle size and zeta potential are not appropriate for prediction due to the lack of significance and fit of some models. Consequently, only %EE could be predicted from this mixture design model.

All formulations prepared from the simplex-centroid mixture design (Table 4 and 5) were translucent and stable showing %EE ranged from 32% to 59%. Particle sizes were in the range from 226 nm to 327 nm. Zeta potentials were in the range from -45 mV to -26 mV. As a result, F9 was found to be the best nanostructured lipid carrier (NLC) with high %EE, small particle size and stable formulation with high negative zeta potential. Thus, this formulation was further development of EWH-NLC cream.

Table 4. Formulation compositions for simplex-centroid mixture design

Ingredients	F1 from Plackett-Burman design (g)
EWH	0.1
Glyceryl monostearate (GMS)	X_1
Stearic acid (SA)	X_2
Isopropyl Myristate (IPM)	X_3
Sorbitan oleate (Span80)	0.6
Polysorbate 80 (Tween80)	6
DI water part I	0.2
DI water for solidification	$100-(\Sigma X_i+0.1+0.2+0.6+6)$
Total	100

Table 3. Layout of Plackett-Burman design

Standard number of formulation	A = Glyceryl monostearate (GMS) (g)	B = Stearic acid (SA) (g)	C = Cetyl alcohol (CA) (g)	D = Isopropyl myristate (IPM) (g)	E = Polysorbate 80 (Tween 80) (g)	F = Sorbitane monooleate (Span 80) (g)	% Entrapment efficiency (%EE) (Y_1)	Particle size (nm) (Y_2)	Zeta potential (Y_3)
1	0.3	0.3	0.0	0.6	6.0	0.6	70.59	183.17	-27.96
2	0.0	0.3	0.3	0.3	6.0	0.6	34.79	169.57	-25.96
3	0.3	0.0	0.3	0.6	0.0	0.6	unstable	unstable	unstable
4	0.0	0.3	0.0	0.6	6.0	0.0	27.56	1199.33	-16.83
5	0.0	0.0	0.3	0.3	6.0	0.6	60.45	245.47	-24.01
6	0.0	0.0	0.0	0.6	0.0	0.6	unstable	unstable	unstable
7	0.3	0.0	0.0	0.3	6.0	0.0	57.04	210.17	-17.75
8	0.3	0.3	0.0	0.3	0.0	0.6	unstable	unstable	unstable
9	0.3	0.3	0.3	0.3	0.0	0.0	unstable	unstable	unstable
10	0.0	0.3	0.3	0.6	0.0	0.0	unstable	unstable	unstable
11	0.3	0.0	0.3	0.6	6.0	0.0	55.31	701.10	-16.12
12	0.0	0.0	0.0	0.3	0.0	0.0	0	715.33	-10.82

Table 5. Optimization of formulations variables for nanostructured lipid carriers (NLC)

Standard number	GMS (A)	SA (B)	IPM (C)	%EE (Y_1)			Particle size (nm) (Y_2)			Zeta potential (Y_3)		
				AVG		SD	AVG		SD	AVG		SD
1	0.6	0.3	0.6	49.36	±	3.64	266.7	±	3.40	-28.49	±	0.72
2	0.3	0.6	0.6	43.11	±	2.41	326.4	±	4.39	-26.91	±	0.28
3	0.3	0.3	0.9	31.70	±	2.04	226.8	±	2.41	-38.94	±	0.40
4	0.45	0.45	0.6	56.71	±	6.74	252.0	±	3.50	-45.43	±	0.77
5	0.45	0.3	0.75	57.18	±	0.72	228.6	±	5.21	-35.45	±	1.02
6	0.3	0.45	0.75	54.05	±	8.85	248.7	±	2.87	-27.24	±	0.59
7	0.4	0.4	0.7	54.52	±	4.55	239.5	±	3.70	-44.87	±	0.49
8	0.5	0.35	0.65	54.83	±	8.93	243.0	±	3.66	-33.05	±	3.87
9	0.35	0.5	0.65	59.21	±	8.51	233.7	±	3.54	-41.26	±	1.46
10	0.35	0.35	0.8	44.05	±	5.79	247.7	±	1.00	-34.62	±	1.79
11	0.3	0.3	0.9	35.76	±	1.35	232.9	±	3.80	-38.54	±	0.03
12	0.3	0.45	0.75	56.40	±	5.27	250.5	±	6.18	-31.95	±	0.89
13	0.6	0.3	0.6	47.33	±	2.75	253.0	±	2.66	-36.84	±	0.40
14	0.3	0.6	0.6	46.39	±	3.12	327.3	±	8.23	-40.66	±	8.00

The responses of formulation and processing variables on %EE of EWH-NLC was proposed from the simplex-centroid mixture design model for entrapment efficiency of EWH-NLC in equation (8):

$$Y1 = -211.84X_1 - 287.54\ X_2 - 184.48X_3 + 373.68X_1X_2 + 528.49X_1X_{3*} + 639.26X_2X_{3*} \quad (8)$$

There were positively interaction of GMS and IPM (X_1X_3), and SA and IPM (X_2X_3) resulting in higher %EE. The response surface plots in Figure 1A showed that % EE increased with appropriate proportions of GMS (X_1), SA (X_2) and IPM (X_3). Numerical optimization analysis showed an appropriate proportion of parameters, preferably at 0.964, to get the highest %EE at 58.22 % using 0.42 g GMS, 0.42 g SA and 0.67 g IPM.

3.3 Model validation

The optimized formulations attained by the graphical optimization were prepared to validate predicted results. The yellow area in the overlay plot, showed in Figure 1B, was the area of the desired formulation criteria. This area was chosen from the actual results in optimization formulation study, that were the high %EE ranged from 55 to 59%, the small particle size ranged from 225 to 265 nm and the high negative zeta potential in a range of -45 to -30 mV. F9 and another four formulations were chosen from yellow area of overlay plot. The amount of each parameter in formulations and % prediction error are shown in Table 6. The observed values of all responses were comparable with the prediction values. Since all responses had a % prediction error lower than 10%, it was confirmed that the model used for prediction was reliable for the optimization procedure.

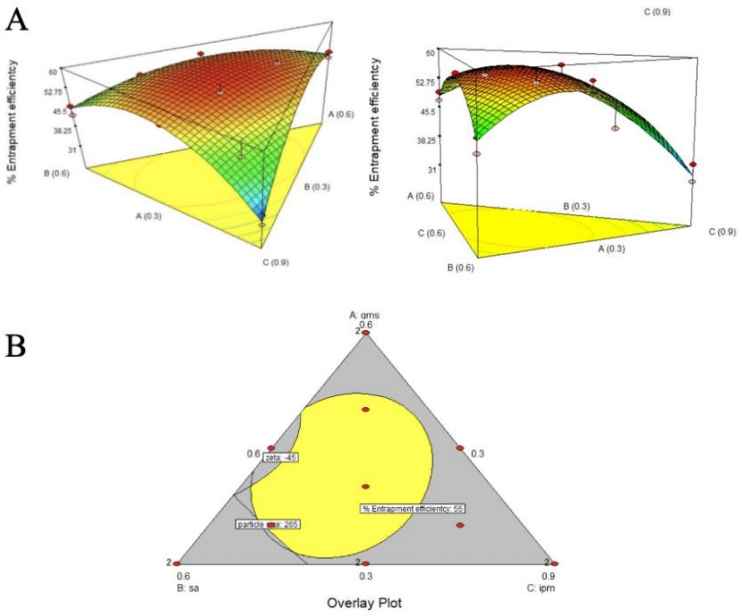

Figure 1. Response surface plots showing the effects of variables on %EE of EWH-NLC (A); The overlay plot from optimization process (B)

Table 6. Model validation

Formu-lation	GMS	SA	IPM	% EE			Particle size (nm)			Zeta potential (mV)		
				Observe value	Prediction value	Prediction error (%)	Observe value	Prediction value	Prediction error (%)	Observe value	Prediction value	Prediction error (%)
1 (F9)	0.35	0.50	0.65	59.21±8.51	56.89	3.92	233.70±3.54	252.11	7.30	-41.26±1.46	-38.30	7.17
2	0.51	0.37	0.62	53.63±2.38	55.41	3.21	227.15±4.45	238.66	4.82	-33.44±0.59	-31.94	4.70
3	0.44	0.34	0.72	53.96±4.13	55.82	3.34	248.00±1.41	238.65	3.92	-32.97±2.65	-35.23	6.43
4	0.35	0.41	0.74	57.82±1.93	56.06	1.93	238.95±1.06	237.37	0.67	-33.57±0.54	-35.61	5.73
5	0.42	0.39	0.69	58.95±0.28	58.02	0.28	234.25±5.30	236.31	0.87	-41.49±3.23	-39.13	6.02

3.4 Anti-inflammation activity using nitric oxide inhibition assay

RAW 264.7 cells cytotoxic study revealed that empty-NLCs and EWH-NLC exhibited cytotoxicity at the concentrations of 250 µg/ml and 500 µg/ml (data not shown). Figure 2 shows that The empty-NLC in the concentrations of 1.95-125 µg/ml did not significantly reduce NO production. However, EWH-NLC in the concentrations of 31.25-125 µg/ml possessed a significant inhibition of the nitrite accumulation in LPS-stimulated RAW 264.7 cells in a dose-dependent manner in comparison to LPS alone. The EWH-NLC at 125 µg/ml possessed the highest NO inhibition.

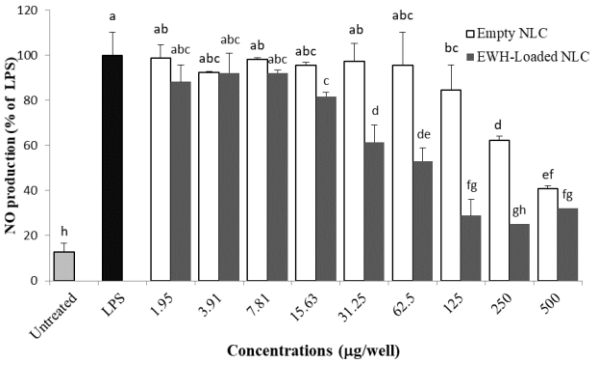

Figure 2. Effect of different concentrations of EWH-NLC and empty NLC on LPS-induced nitric oxide in RAW 264.7 macrophages. Value with different alphabets (a-h) indicated significant differences *(p<0.05)*.

3.5 *In vitro* release assay

Table 7 demonstrated that the release kinetics profiles of EHW in a vehicle, EWH and EWH-NLC from cream base were best fitted with the Higuchi kinetic model with R^2=0.9257, 0.7764 and 0.9223, respectively (Figure 3, Table 7). EWH in solution showed 56.59 ± 4.87 % release in 720 min (12 hrs), that was significantly faster than the release of EWH (34.54 ± 1.86%) and EWH-NLC from cream (28.19 ± 4.12 %). EWH-NLC from cream exhibited sustained release profile.

Table 7. *In vitro* release kinetics model

	Zero order (R^2)	First order (R^2)	Higuchi (R^2)
EWH in solution	0.7926	0.5105	0.9257
EWH-NLC in cream base	0.8108	0.6138	0.9223
EWH in cream base	0.5489	0.3996	0.7764

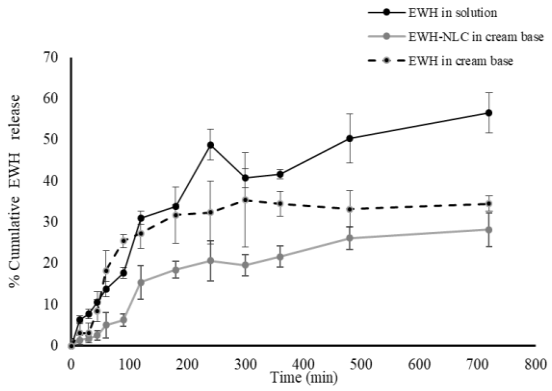

Figure 3. Release profiles of EWH and EWH-NLC in solution and cream base

4. Discussion

It is evident that %EE significantly increased with the increase of lipid concentration due to the ability of higher content of lipid to provide more space for accommodation of hydrolysates and reducing drug diffusion into external phase. Moreover, GMS, exhibiting emulsifying properties, have an ability to adsorb active ingredient on its surface resulting in higher %EE. Increase of GMS and Span 80 concentrations and decrease of IPM concentrations resulted in significant reduction of particle size. At the same time, increase of the lipid content caused particle size enlargement. It was probably due to the reduction of emulsifying efficiency that was a direct cause of the particle agglomeration. In addition, Tween 80 and Span 80 reduced interfacial tension and facilitated homogenization of lipid in the aqueous phase, and consequently formation of smaller particles. IPM was used as liquid lipid to obtain imperfect lipid matrix structure capable of accommodation of larger amount of drug molecules. Despite the presence of liquid lipid, NLC matrix remained in the solid stage at room temperature by controlling the content of liquid lipid (Üner, Karaman, & Aydoğmuş, 2014). Increase of IPM amount made NLC structure unstable leading to particle agglomeration with the following increase of the particle size. However, NLCs surface charge, and the additional charges created by surfactants or stabilizer molecules in the Stern layer resulted in increasing negative value of zeta potential of NLCs that made the formulation more stable (Kovacevic, Savic, Vuleta, Müller, & Keck, 2011).

Formulation optimization study indicated that interaction effects between GMS and IPM, and SA and IPM had positive influence on %EE. This suggested that increased lipid concentration also resulted in higher %EE. This may be due to the higher concentration of lipid that can potentially provide more space to increment active content and reduce escaping of drug into the external phase. GMS exhibited an emulsifying effect resulting in protection of active ingredient inside and adsorption on their surface. Comparing to GMS, SA is a long chain saturated fatty acid enhancing matrix of NLC and protecting drug diffusion to external phase (Shah et al., 2016). Moreover, increased concentrations of liquid lipid in solid lipid resulted in formation of amorphous solid structures that help to improve drug loading and decrease its expulsion from the matrix during storage period simultaneously increasing %EE.

Results of anti-inflammatory activity of EWH-NLC in LPS-stimulated RAW 264.7 cells demonstrated that empty-NLCs and EWH-NLC exhibited cytotoxicity at the concentrations of 250 µg/ml and 500 µg/ml. It might be possible that stearic acid in NLCs at high concentrations inhibits NO production by damaging RAW cells' membrane integrity and/or increase of DNA fragmentation causing cell death as reported by de Lima, de Sa Lima, Scavone, and Curi (2006). However, at 125 µg/ml, EWH-NLC exhibited a good anti-inflammatory activity with the effective inhibition of NO production by 71.1% while empty-NLC could inhibit NO production only by 15.5%. This might be due to EWH-NLC having a smaller particle size compared to non-entrapment EWH are able to increase the interfacial surface area and enhance the amount of active compound delivery into the cell.

EWH in solution showed faster release than EWH and EWH-NLC in cream base. This could be attributed to EWH in PBS solution that can easily diffuse into aqueous medium. EWH-NLC in cream exhibited a sustained-release profile that could be attributed to the slow diffusion of EWH from NLC dispersed in cream base due to the ability of NLC to entrap EWH inside and adsorb the compounds on their surface. The release behavior of EWH-NLC showed the best fit to Higuchi model indicating a diffusion-controlled mechanism of release. The initial occurrence of faster release clearly indicates the location of EWH adsorbed on the surface of NLC. Subsequently, EWH might slowly diffuse from the core of the lipid particle to its medium.

5. Conclusions

Mixture design could be used to optimization the EWH-NLC entrapment demonstrating anti-inflammation activity by inhibition NO production. The release profile from EWH-NLC formulation exhibited sustained-release profile with Higuchi model. These results indicate that the NLC is suitable carrier for topical application of EWH. Moreover, the design of experiment applied for optimization of NLCs formulation development is a good tool to save time and cost in formulation development. Further studies on cosmetic applications of EWH-NLC could be worth investigation.

Acknowledgements

This work was supported by a grant from the National Research Council of Thailand, (grant number B05F630053).

References

Bradford, M. M. (1976). A rapid and sensitive method for the quantitation of microgram quantities of protein utilizing the principle of protein-dye binding. *Analytical Biochemistry*, *72*, 248–254.

Czajkowska-Kośnik, A., Szekalska, M., & Winnicka, K. (2019). Nanostructured lipid carriers: A potential use for skin drug delivery systems. *Pharma cological Reports*, *71*(1), 156–166.

de Lima, T. M., de Sa Lima, L., Scavone, C., & Curi, R. (2006). Fatty acid control of nitric oxide production by macrophages. *FEBS Letters*, *580*(13), 3287–3295.

Fischer, D., Li, Y., Ahlemeyer, B., Krieglstein, J., & Kissel, T. (2003). In vitro cytotoxicity testing of polycations: Influence of polymer structure on cell viability and hemolysis. *Biomaterials*, *24*(7), 1121–1131.

Jearranaiprepame, S., Jangpromma, N., & Khunkitti, W. (2019). *Anti-aging bioactivities of egg white hydrolysates*. *Songklanakarin Jornal of Science and Technology*, *41*(4), 924-933.

Jia, L.-J., Zhang, D.-R., Li, Z.-Y., Feng, F.-F., Wang, Y.-C., Dai, W.-T., . . . Zhang, Q. (2010). Preparation and characterization of silybin-loaded nanostructured lipid carriers. *Drug Delivery*, *17*(1), 11–18.

Kovacevic, A., Savic, S., Vuleta, G., Müller, R. H., & Keck, C. M. (2011). Polyhydroxy surfactants for the formulation of lipid nanoparticles (SLN and NLC): Effects on size, physical stability and particle matrix structure. *International Journal of Pharmaceutics*, *406*(1–2), 163–172.

Li, B., & Ge, Z.-Q. (2012). Nanostructured lipid carriers improve skin permeation and chemical stability of idebenone. *AAPS PharmSciTech*, *13*(1), 276–283.

Loo, C., Basri, M., Ismail, R., Lau, H., Tejo, B., Kanthimathi, M., . . . Choo, Y. (2013). Effect of compositions in nanostructured lipid carriers (NLC) on skin hydration and occlusion. *International Journal of Nanomedicine*, *8*, 13–22.

Shah, N. V., Seth, A. K., Balaraman, R., Aundhia, C. J., Maheshwari, R. A., & Parmar, G. R. (2016). Nanostructured lipid carriers for oral bioavailability enhancement of raloxifene: Design and in vivo study. *Journal of Advanced Research*, *7*(3), 423–434.

Shah, P. P., Desai, P. R., Channer, D., & Singh, M. (2012). Enhanced skin permeation using polyarginine modified nanostructured lipid carriers. *Journal of Controlled Release: Official Journal of the Controlled Release Society*, *161*(3), 735–745.

Üner, M., Karaman, E., & Aydoğmuş, Z. (2014). Solid lipid nanoparticles and nanostructured lipid carriers of Loratadine for topical application: Physicochemical stability and drug penetration through rat skin. *Tropical Journal of Pharmaceutical Research*, *13*(5), 653.